SOVIET PHYSICS JETP VOLUME 36, NUMBER 3 MARCH, 1973

# *OPTICAL CONSTANTS AND ELECTRONIC CHARACTERISTICS OF TITANIUM*

I. D. MASH and G. P. MOTULEVICH

P. N. Lebedev Physics Institute, Academy of Sciences of the USSR

Submitted March 1, 1972

Zh. Eksp. Teor. Fiz. 63, 985–992 (September, 1972)

Optical constants of electrolytically polished titanium were determined in the spectral range $\lambda = 0.4–10\ \mu$. The following characteristics were also determined: the conduction-electron density $N = 0.63 \times 10^{22}$ cm$^{-3}$; the effective frequency of collisions between the conduction electrons $\nu = 1.9 \times 10^{14}$ sec$^{-1}$; the electron-phonon interaction constant $\lambda_{\text{eph}} = 0.34$; the Fourier components of the pseudopotential $|V_{1\bar{1}0,1}| = 0.59$ eV, $|V_{1\bar{1}0,0}| = 0.82$ eV, $|v_{1\bar{1}0,2}| = 1.15$ eV.

OPTICAL investigations carried out in a wide range of wavelengths can yield information on the electronic characteristics of metals (see, for example,[1-4]). The present paper describes measurements of the optical constants of Ti in the infrared and visible parts of the spectrum and determination of the electronic characteristics of this metal. Titanium is of interest because it is a component of a series of superconducting alloys with high critical parameters.[5] Moreover, titanium is a transition metal and investigations of the optical band-band transitions can give information on the hybridization of the s and d states of the valence electrons. Measurements of the optical constants were carried out on electrolytically polished bulk polycrystalline samples. Electrolytic polishing was employed because samples used in previous investigations[6-10] were polished mechanically and this distorted the surface layer.

## EXPERIMENTAL PROCEDURE

We prepared three samples of $78 \times 15 \times 6$ mm dimensions by the electron-beam melting method. The purity of the original material was 99.99%. The samples were polished electrolytically in a solution consisting of 850 ml of $H_2SO_4$, 200 ml of HF, and 50 ml $H_2O$. The solution was kept at 45°C and the electropolishing treatment lasted 1 min. The current density during this treatment was 2 A/cm$^2$. The electropolishing treatment removed a layer 200 $\mu$ thick. The specular surfaces obtained in this way were homogeneous.

The optical constants n and $\kappa$ ($n - i\kappa$ is the complex refractive index) were measured by the null polarization method at room temperature. The reflection coefficient of Ti was found to be small and, therefore, light was reflected once from the investigated samples. The measurements in the infrared range were carried out using the apparatus described in[2,11]. One titanium and three gold mirrors were used (the optical constants of these mirrors were determined in preliminary measurements). The measurements in the visible region were carried out using the apparatus described in[2,12].

The results obtained, which are averages of several series of measurements, are given in Table I and in Figs. 1a and 1b. A special check was made of the stability of the optical constants. Small changes in n and $\kappa$, of the order of 2–5%, were observed only after three days from the electropolishing treatment. The experimental error in n and $\kappa$ was deduced from the scatter of the results obtained in different series of measurements. The highest precision was reached in the $\lambda = 0.6–0.8\ \mu$ range, in which the largest number of measurements was carried out: here, the rms error was 0.5% for n and 0.2% for $\kappa$. In the 0.4–0.6 $\mu$ range the errors were 3% for n and 0.7% for $\kappa$; in the 0.8–1 $\mu$ range they were 0.9% for n and 0.5% for $\kappa$; and in the 1–10 $\mu$ range, they were 3–4% for n and 2–4% for $\kappa$.

The dependences $n(\lambda)$ and $\kappa(\lambda)$ ($\lambda$ is the wavelength of light) show that in the long-wavelength range ($\lambda \geq 5\ \mu$) the optical constants are dominated by the conduction-electron contribution; in the 2–5 $\mu$ range a significant contribution is made also by the band-band transition; in the $\lambda < 2\ \mu$ range the band-band transitions predominate. Figure 1 includes also the data taken from[6-8].[1] We can see that the long-wavelength values of $\kappa$ given in these papers are practically identical with our values, whereas at short wavelengths the differences exceed the experimental error. Our values of n disagree with those given in[6-8] throughout the investigated range of wavelengths. Similar results are given in[9,10] but only in the form of dependences of $n^2 - \kappa^2$ and $2n\kappa$ on $\lambda$. The coordinate scales used in these papers have not been chosen happily and, therefore, the values of n and $\kappa$ can be deduced from the graphs only with a considerable error. For this reason we have not included the results of[9,10] in Fig. 1. All that we can say is that the results in these two papers differ more from our values than do the results given in[6-8]. We think that the discrepancies between our values and those given in[6-8] are related to the method used in the preparation of the samples. Mechanical grinding or polishing was used in[6-10] and this treatment produces a cold-worked layer.

## ANALYSIS OF RESULTS

1. At room temperature titanium exhibits the normal skin effect and we can use these standard Drude-Zener formulas.[1,2] However, since the contribution of the

---

[1] In the visible range there is some divergence between the values of n and $\kappa$ reported in [7] and in [8]. We shall use the results given in [8].

Table I. Optical constants of titanium

| λ, μ | n | ϰ | λ, μ | n | ϰ | λ, μ | n | ϰ | λ, μ | n | ϰ |
|---|---|---|---|---|---|---|---|---|---|---|---|
| 0,40 | 1,71 | 2,23 | 0,635 | 2,49 | 3.11 | 0,895 | 3,24 | 3,51 | 3,5 | 3,35 | 6,40 |
| 0,42 | 1,73 | 2,44 | 0,655 | 2,55 | 3,15 | 0,92 | 3,30 | 3,54 | 4.0 | 3,31 | 7.33 |
| 0,44 | 1,89 | 2.59 | 0,675 | 2,60 | 3,17 | 0,94 | 3,34 | 3.55 | 4.5 | 3,36 | 8,30 |
| 0,46 | 1,92 | 2,67 | 0.70 | 2.67 | 3.20 | 0.96 | 3,40 | 3.55 | 5.0 | 3,44 | 9.37 |
| 0,48 | 2,03 | 2.77 | 0,72 | 2.73 | 3.22 | 0.98 | 3.42 | 3,58 | 5,5 | 3,57 | 10.1 |
| 0,50 | 2,10 | 2,82 | 0,74 | 2,78 | 3.23 | 1,2 | 3,30 | 3.70 | 6.0 | 3,80 | 10.9 |
| 0.52 | 2,19 | 2,88 | 0,765 | 2,83 | 3,30 | 1.5 | 3,54 | 4.00 | 7,0 | 4.56 | 12.7 |
| 0,54 | 2,22 | 2.91 | 0,785 | 2.91 | 3,34 | 1,8 | 3.89 | 4,29 | 8,0 | 5.81 | 14.9 |
| 0.56 | 2.27 | 2,94 | 0.810 | 2,98 | 3.40 | 2,0 | 4,03 | 4.47 | 9,0 | 7,27 | 16,1 |
| 0.57 | 2,31 | 2,98 | 0.830 | 3.06 | 3.44 | 2,25 | 4,02 | 4,52 | 10,0 | 9,09 | 18,6 |
| 0.59 | 2,36 | 3,00 | 0,855 | 3,13 | 3,49 | 2.5 | 3,96 | 4,60 | | | |
| 0,61 | 2.42 | 3,04 | 0,875 | 3,18 | 3,51 | 3.0 | 3,65 | 5,36 | | | |

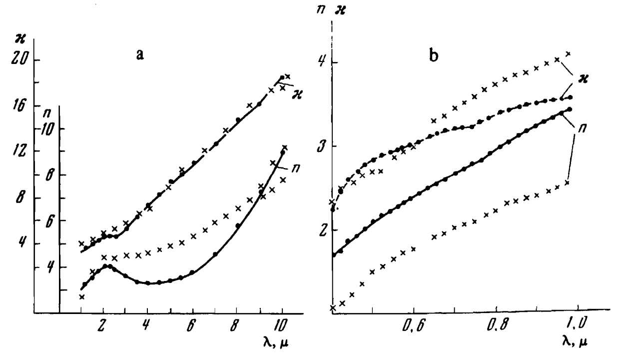

FIG. 1. Dependences of n and κ on λ: a– in the 1-10 μ region, ●–present investigation, X–results reported in [6-8]; b–in the 0.4-1 μ region, ●–present investigation, X–results reported in [8].

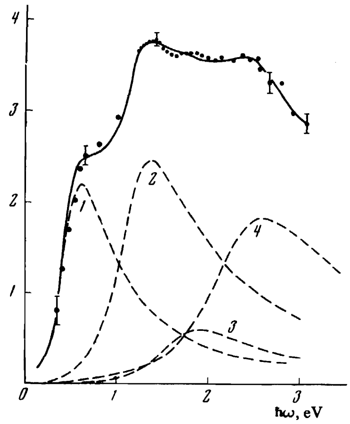

FIG. 2. Separation of a complex optical band due to band-band transitions into its components: ●–experimental values of $\sigma_b$; the dashed curves represent the values of $\sigma_b(\omega)$ of bands 1, 2, 3, and 4; the continuous curve is the sum $\sum_{i=1}^{4}\sigma_{bi}(\omega)$ of bands 1, 2, 3, and 4.

conduction electrons to $\epsilon_1$ ($\epsilon = \epsilon_1 - i4\pi\sigma/\omega$ is the complex permittivity) is much smaller than for other metals, the contribution of the virtual band-band transitions to this quantity is quite considerable. We shall determine the conduction-electron density N and the effective frequency of collisions from the values of n and κ in the spectral range 5–10 μ. The principal band-band transitions in Ti are observed in the visible and near infrared regions. Therefore, the virtual band-band transitions in the selected spectral range (5–10 μ) make a contribution to $\epsilon_1$ which is independent of the frequency ω. This contribution can be determined from the Kramers-Kronig relationship.[13] Thus, we shall use the relationships:

$$\varepsilon_1-\varepsilon_0=-\frac{4\pi e^2}{\omega^2+\nu^2}\frac{N}{m},\quad \varepsilon_0=8\int\frac{\sigma_b(\omega)}{\omega^2}d\omega, \tag{1}$$

$$\sigma=\frac{e^2\nu}{\omega^2+\nu^2}\frac{N}{m}. \tag{2}$$

Here, σ is the conductivity at the frequency ω; ω is the angular frequency of light; e and m are the charge and mass of a free electron; $\epsilon_0$ is the contribution of the virtual band-band transitions. We shall take N and ν to be the average values in the selected frequency range: these values are $N = (0.63 \pm 0.05) \times 10^{22}$ cm$^{-3}$, $\nu = (1.9 \pm 0.05) \times 10^{14}$ sec$^{-1}$. The contribution of the virtual band-band transitions is represented by $\epsilon_0 \approx 26$.

The values of N and $\sigma_{st}(T)$ can be used to determine the electron-phonon interaction constant $\lambda_{eph}$ from the formulas[14]

$$\lambda_{eph}=\frac{\hbar}{2\pi k_B}\frac{\nu_{eph}(T)}{T},\quad \nu_{eph}(T)=\frac{e^2}{\sigma_{st}(T)}\frac{N}{m}. \tag{3}$$

Here, $\nu_{eph}(T)$ is the classical frequency of collisions of electrons with phonons at a temperature T; $\sigma_{st}(T)$ is the static conductivity at the same temperature T; $k_B$ is the Boltzmann constant. The formulas in Eq. (3) are valid in the range of temperatures in which the ratio $\nu_{eph}(T)/T$ is independent of T.

According to[15], this ratio is practically constant in the temperature range 273–573°K. In this range $\sigma_{st}(T) \approx 5.5 \times 10^6\ \Omega^{-1}\cdot$cm$^{-1}$. If we use this value, we find that $\lambda_{eph} = 0.34$, which is in agreement with 0.38 obtained in[16] from the superconducting characteristics of Ti.

2. We shall use the optical constants in the $\lambda < 5$ μ range to study the band-band conductivity $\sigma_b = \sigma_{exc} - \sigma_e$, where the subscripts b and e refer to the band-band transitions and to the conduction electrons, respectively. The conductivity $\sigma_e$ can be found from Eq. (2). The values of $\sigma_b$ plotted in Fig. 2 are denoted by points. It is evident from Fig. 2 that a complex band $\sigma_b(\omega)$ is observed in the $\hbar\omega = 0.3$–$3.1$ eV range and this band consists of at least four simple bands. This structure of the $\sigma_b(\omega)$ band was the same in all ten series of measurements. We separated the simple bands using their profiles obtained in[17]. The results of this separation are shown as dashed curves in Fig. 2. The continuous curve is the sum of all four simple bands. The parameters of the bands are listed in Table II, where the following notation is employed: $\omega_{max}$ is the frequency of the band maximum; ν′ is the dimensionless relaxation parameter introduced in[17]; $\sigma_{max} = \sigma_b(\omega_{max})$; $\hbar\omega_g$ is the energy gap associated with a given band. Since the relaxation time is short,

Table II. Parameters of experimentally observed optical bands due to band-band conduction in titanium

| Band No. | max, eV | $\nu'$ | $\sigma_{max}$, $10^{15}$ sec$^{-1}$ | $\hbar\omega_g$, eV |
|---|---|---|---|---|
| 1 | 0.63±0.05 | 0,50±0,1 | 2,2±0.2 | 0.47±0.08 |
| 2 | 1,40±0,1 | 0,30±0,05 | 2.46±0,2 | 1.18±0.14 |
| 3 | 1,9±0,1 | 0,25±0,05 | 0.6±0,2 | 1.65±0,18 |
| 4 | 2.6±0,1 | 0,25±0,05 | 1,82±0,2 | 2,3±0,21 |

$\hbar\omega_g$ is much smaller than $\hbar\omega_{max}$. The values of $\hbar\omega_g$ were calculated from the experimental values of $\omega_{max}$ and $\nu'$ using the formulas given in[17].

## DISCUSSION OF RESULTS

Titanium is a tetravalent metal ($3d^2 4s^2$) with the hcp lattice. The ratio of the lattice constants is $c/a = 1.59$; $a = 295$ Å.[18] since the phase volume of the valence electrons is fixed, the average Fermi momentum $p_F$ of the hybridized s and d electrons should be close to the Fermi momentum of a sphere of free electrons $p_F^0$ if the density of these electrons is close to the valence value. In the case of titanium, $p_F^0 = 0.885$. The values of the momenta will always be given in units of $2\pi\hbar/a$. If the quoted value of the momentum $p_F$ is correct, the Fermi surface should intersect four systems of the Bragg planes and five systems of the lines of intersection of the Bragg planes, listed in Table III. This table includes also the number of physically equivalent planes or lines of intersection $n_g$ and their distances $d_g$ from the center of the Brillouin zone, which is the point Γ. The distances $d_g$ of the lines of intersection are expressed in terms of the distances to the nearest Bragg planes $P_g$; here, g is the index of the Bragg plane and of the corresponding Fourier component of the pseudopotential. For the hcp lattice,[19] we have

$$p_{1\bar{1}0,0} = \frac{1}{\sqrt{3}}, \quad p_{000,2} = \frac{a}{c},$$

$$p_{1\bar{1}0,1} = \frac{1}{2}\sqrt{\frac{4}{3} + \left(\frac{a}{c}\right)^2} \quad p_{1\bar{1}0,2} = \sqrt{\frac{1}{3} + \left(\frac{a}{c}\right)^2}.$$

The band-band transitions associated with the Bragg planes are usually characterized by a much higher combined band-band density of states than the transitions associated with the lines of intersection of these planes. Correspondingly, the intensity of the optical bands associated with the former transitions is much higher than the intensity of the optical bands associated with the latter transitions. We shall refer to these optical bands as the first- and second-order bands.[2)] The energy gaps for the first- and second-order optical bands are related to the Fourier components of the pseudopotential $V_g$. These gaps are also listed in Table III. The energy gaps for the optical bands associated with the lines of intersection of the Bragg planes of an hcp metal can be calculated as described in[20]. The last row in Table III represents the data for a line of intersection of three planes. The lines of intersection of the $\{1\bar{1}0,0\}$, $\{10\bar{1},1\}$ and $\{1\bar{1}0,1\}$, $\{10\bar{1},1\}$ planes are separated by the same distances from the point Γ and have the same energy gaps. The same is also true of the lines of intersection of the $\{1\bar{1}0,1\}$, $\{000,2\}$ and $\{1\bar{1}0,1\}$, $\{1\bar{1}0,\bar{1}\}$ planes.

We shall identify the observed optical bands of the band-band conductivity using the relationship $V_g = U_g S_g$.[22] Here, $U_g$ is the form factor and $S_g$ is the structure factor. We shall estimate $U_g$ from the results obtained by Arkhipov.[23] No difficulties are encountered in the calculation of $S_g$, which can be performed by the standard method.[24] In this way we obtain $2V_{1\bar{1}0,2} = 2.3$ eV; $2V_{1\bar{1}0,0} = -2.1$ eV, $2V_{000,2} = -2.8$ eV; $2V_{1\bar{1}0,1} = -1.7$ eV. If we compare these results with the energy gaps associated with the experimentally observed optical bands, we can attribute band 2 to $\{1\bar{1}0,1\}$, band 3 to $\{1\bar{1}0,0\}$, and band 4 to $\{1\bar{1}0,2\}$. The $\{000,2\}$ band lies at the edge of the investigated range of wavelengths where the measurements are not very accurate. Evidently, it appears as a small singularity in the dependence $\sigma_b(\omega)$ which has a maximum at $\hbar\omega_{max} \approx 2.83$ eV. The attribution made above is in agreement with the intensities of the optical bands, which should be proportional to $n_g p_g$. The largest areas under the spectral profiles are obtained for bands 2 and 4, for which $n_g = 12$ and $p_g/p_F = 0.74$ and 0.96, respectively. In the case of band 3, we have $n_g = 6$ and $p_g/p_F = 0.65$. The area of this band is less than the areas of bands 2 and 4. The $\{000,2\}$ band, for which $n_g = 2$ and $p_g/p_F = 0.71$, has the smallest area. Additional data which would help in the identification of the bands can be obtained from optical measurements on oriented single crystals. If we adopt the identification made above, we obtain the following values of the Fourier components of the pseudopotential: $|V_{1\bar{1}0,1}| = 0.59 \pm 0.07$ eV, $|V_{1\bar{1}0,0}| = 0.82 \pm 0.09$ eV, $|V_{1\bar{1}0,2}| = 1.15 \pm 0.10$ eV, $|V_{000,2}|$ is approximately equal to 1.2 eV.[3)]

These results can be used to calculate the frequencies of the second-order bands, listed in Table IV. The second-order bands with gaps of 0.31, 0.47, 0.61, and 0.77 eV overlap and combine giving rise to an average energy gap which is approximately 0.49 eV.[4)] This complex band can be identified with the experimentally observed band 1, for which the energy gap is 0.47 eV and which is characterized by a large value of the dimensionless relaxation parameter $\nu'$ (this large value is also evidence of the complex structure of this band). The large area of band 1 is due to the fact that about 80 lines of intersection contribute to this band. The bands with gaps of 3.9 and 4.7 eV also overlap and give rise to a common band with an average gap of 4.3 eV. A band with $\hbar\omega_{max} \approx 5$ eV is reported also in[7]. If we estimate $\nu'$ from the width of this band, we find that $\nu' = 0.25$. The corresponding energy gap is $\hbar\omega_g = 4.3$ eV. The agreement between the energy gaps allows us to identify this optical band with the sum of two second-order bands considered above. The other second-order bands with gaps of 1.2, 1.9, 2.0, 2.2, 2.5, 2.8, and 2.9 eV are located within the principal complex band which

---

[2)] In our investigation reported in [21] the second-order optical bands are called the combination bands.

[3)] We assumed that $\hbar\omega_{max} \approx 2.83$ eV, $\nu' = 0.25$ for the {000, 2} band.

[4)] In calculation of the average value we assumed that the intensity of the second-order lines was proportional to $n_g$.

**Table III.** Optical bands due to band-band conduction associated with Bragg planes and lines of intersection of such planes in hcp lattice

| Planes | $n_g$ | $d_g$ | $\frac{d_g^{**}}{p_F^0}$ | Energy gaps |
|---|---|---|---|---|
| $\{1\bar{1}0.0\}$ | 6 | $p_{1\bar{1}0.0}$ | 0.652 | $2\lvert V_{1\bar{1}0.0}\rvert$ |
| $\{000.2\}$ | 2 | $p_{000.2}$ | 0.711 | $2\lvert V_{000.2}\rvert$ |
| $\{1\bar{1}0.1\}$ | 12 | $p_{1\bar{1}0.1}$ | 0.742 | $2\lvert V_{1\bar{1}0.1}\rvert$ |
| $\{1\bar{1}0.2\}$ | 12 | $p_{1\bar{1}0.2}$ | 0.965 | $2\lvert V_{1\bar{1}0.2}\rvert$ |
| Lines of intersection of planes | | | | |
| $\{1\bar{1}0.0\}$, $\{1\bar{1}0.1\}$ | 12 | $p_{1\bar{1}0.1}$ | 0.742 | $\lvert 2\lvert V_{1\bar{1}0.0}\rvert \pm 2\lvert V_{1\bar{1}0.1}\rvert\rvert$<br>$2\lvert V_{1\bar{1}0.1}\rvert$ |
| $\{1\bar{1}0.0\}$, $\{10\bar{1}.0\}$ | 6 | $\frac{2}{\sqrt{3}} p_{1\bar{1}0.0}$ | 0.752 | $3\lvert V_{1\bar{1}0.0}\rvert$ |
| $\{1\bar{1}0.0\}$, $\{10\bar{1}.1\}$ | 24 | | | $2R_1$**** |
| $\{1\bar{1}0.1\}$, $\{10\bar{1}.1\}$ | 12 | $p$*** | 0.826 | $\lvert {}^3/_2\lvert V_{1\bar{1}0.0}\rvert \pm R_1\rvert$ |
| $\{1\bar{1}0.1\}$, $\{000.2\}$ | 12 | $\frac{p^2_{1\bar{1}0.0}}{p_{1\bar{1}0.0}}$ | 0.847 | $2R_2$<br>$\lvert {}^3/_2\lvert V_{000.2}\rvert \pm R_2$*****$\rvert$ |
| $\{1\bar{1}0.1\}$, $\{1\bar{1}0.\bar{1}\}$ | 6 | | | |
| $\{1\bar{1}0.0\}$, $\{000.2\}$ and $\{1\bar{1}0.2\}$ | 12 | $p_{1\bar{1}0.2}$ | 0.965 | $\lvert 2\lvert V_{1\bar{1}0.2}\rvert \pm 2\lvert V_{1\bar{1}0.0}\rvert\rvert$<br>$\lvert 2\lvert V_{1\bar{1}0.2}\rvert \pm 2\lvert V_{000.2}\rvert\rvert$ |

*This table lists the planes and lines intersecting the Fermi surface for the valence $\eta = 4$.

**The ratios $d_g/p_F^0$ are calculated.

*** $p = p_{1\bar{1}0.1}/[1-(p_{1\bar{1}0.0}/2p_{1\bar{1}0.1})^2]^{1/2}$

**** $R_1 = ({}^1/_4\,|V_{1\bar{1}0.0}|^2 + 2\,|V_{1\bar{1}0.1}|^2)^{1/2}$,

***** $R_2 = ({}^1/_4\,|V_{000.2}|^2 + 2\,|V_{1\bar{1}0.1}|^2)^{1/2}$.

**Table IV.** Frequencies of second-order bands of titanium

| Lines of intersection of Bragg planes | $n_g$ | Frequencies of second-order bands, eV |
|---|---|---|
| $\{1\bar{1}0.0\}$ $\{1\bar{1}0.1\}$ | 12 | 0.47 1.18 2.88 |
| $\{1\bar{1}0.0\}$ $\{10\bar{1}.0\}$ | 6 | 2.48 |
| $\{1\bar{1}0.0\}$ $\{10\bar{1}.0\}$ | 24 | 0,31 1.86 2,17 |
| $\{1\bar{1}0.1\}$ $\{10\bar{1}.1\}$ | 12 | |
| $\{1\bar{1}0.1\}$ $\{000.2\}$ | 12 | 0.77 * 2.05 * 2.82 * |
| $\{1\bar{1}0.1\}$ $\{1\bar{1}0.\bar{1}\}$ | 6 | |
| $\{1\bar{1}0.0\}$ $\{000.2\}$ $\{1\bar{1}0.2\}$ | 12 | 0.61 3.91 4.66 * |

*These frequencies are obtained for an estimated value $|V_{000.2}| = 1.2$ eV.

consists of four first-order bands that cannot be separated by the method employed above. We note that the lines of intersection of the three Bragg planes $\{1\bar{1}0,0\}$, $\{000,2\}$, and $\{1\bar{1}0,2\}$ have an additional small energy gap which is equal to $2\,\|\,V_{000,2}| - |V_{1\bar{1}0,2}\,\|$. However, our experimental data do not allow us to find the value of this gap.

Thus, the observed number of the band-band conductivity bands and the positions of their maxima are in good agreement with the hypothesis of complete hybridization of the s and d electrons in Ti. This hypothesis is also in agreement with the low density of the conduction electrons (0.1 electrons/atom) deduced from the measurements in the infrared part of the spectrum. The low value of N is related to the large number of the Bragg planes intersecting the Fermi surface and to the relatively large values of the corresponding Fourier components of the pseudopotential.

If we assume that s and d electrons are hybridized, the infrared data can be used to estimate the average velocity of electrons on the Fermi surface $v_F$ and the total area of this surface $S_F$ from the relationship[1,2] $v_F/v_F^0 \approx S_F/S_F^0 \approx \sqrt{N/N_{val}}$. Here, the superscript 0 denotes the free-electron value when the density of electrons is equal to the valence density. In the case of titanium we find that $v_F = 0.4 \times 10^8$ cm/sec and that

$$S_F = 8\cdot 10^{-38}\ \mathrm{g^2\cdot cm^2\cdot sec^{-2}},$$

We are grateful to A. I. Golovashkin and A. A. Shubin for making available the apparatus used in measurements of the optical constants and for their valuable advice.

---

[1] G. P. Motulevich, Usp. Fiz. Nauk 97, 211 (1969) [Sov. Phys.-Usp. 12, 80 (1969)].

[2] G. P. Motulevich, Tr. Fiz. Inst. Akad. Nauk SSSR 55, 3 (1971).

[3] A. I. Golovashkin, I. E. Leksina, G. P. Motulevich, and A. A. Shubin, Zh. Eksp. Teor. Fiz. 56, 51 (1969). [Sov. Phys.-JETP 29, 27 (1969)].

[4] A. I. Golovashkin, I. D. Mash, and G. P. Motulevich, Kratk. Soobshch. Fiz. FIAN No. 9, 51 (1970).

[5] J. K. Hulm and R. D. Blaugher, Phys. Rev. 123, 1569 (1961).

[6] G. A. Bolotin, A. N. Voloshinskiĭ, M. M. Kirillova, M. M. Noskov, A. V. Sokolov, and B. A. Charikov, Fiz. Metal. Metalloved. 13, 823 (1962).

[7] M. M. Kirillova and B. A. Charikov, Fiz. Metal. Metalloved. 15, 315 (1963); Opt. Spektrosk. 17, 254 (1964); Fiz. Metal. Metalloved. 19, 495 (1965).

[8] M. M. Kirillova, Kandidatskaya dissertatsiya (Thesis for Candidate's Degree), IFM AN SSSR, Sverdlovsk, 1968.

[9] A. P. Lenham and D. M. Treherne, Proc. Intern. Colloq. on Optical Properties and Electron Structure

of Metals and Alloys, Paris, 1965, publ. by North-Holland, Amsterdam, 1966; J. Opt. Soc. Amer. 56, 1076 (1966).

[10] A. P. Lenham and D. M. Treherne, J. Opt. Soc. Amer. 56, 1137 (1966).

[11] G. P. Motulevich and A. A. Shubin, Opt. Spektrosk., 2, 633 (1957).

[12] A. I. Golovashkin and G. P. Motulevich, Zh. Eksp. Teor. Fiz. 47, 64 (1964) [Sov. Phys.-JETP 20, 44 (1965) (1965)].

[13] L. D. Landau and E. M. Lifshitz, Elektrodinamika sploshnykh sred, GITTL, M., 1957 (Electrodynamics of Continuous Media, Pergamon Press, Oxford, 1960).

[14] E. G. Maksimov and G. P. Motulevich, Zh. Eksp. Teor. Fiz., 61, 414 (1971). [Sov. Phys.-JETP 34, 219 (1972)].

[15] G. W. C. Kaye and T. H. Laby, Tables of Physical and Chemical Constants, 12th ed., Longmans, London, 1959 (Russ. Transl., Nauka Fizmatgiz, M., 1962).

[16] W. L. McMillan, Phys. Rev., 167, 331 (1968).

[17] A. I. Golovashkin and G. P. Motulevich, Zh. Eksp. Teor. Fiz. 57, 1054 (1969) [Sov. Phys.-JETP 30, 575 (1970)]; Preprint No. 76, FIAN, M., 1969; Preprint No. 41, FIAN, M., 1970.

[18] Handbook of Chemistry and Physics, The Chemical Rubber Co., Cleveland, Ohio (1955).

[19] N. F. Mott and H. Jones, The Theory of the Properties of Metals and Alloys, Oxford, Clarendon Press, 1936.

[20] W. A. Harrison, Pseudopotentials in the Theory of Metals, Benjamin, New York, 1966 (Russ. Transl., Mir, M., 1968).

[21] I. D. Mash and G. P. Motulevich, Fiz. Metal. Metalloved. (in press).

[22] J. M. Ziman, Principles of the Theory of Solids, Cambridge University Press, 1964 (Russ. Transl., Mir, M., 1966).

[23] R. G. Arkhipov, Zh. Eksp. Teor. Fiz. 59, 1711 (1970) [Sov. Phys.-JETP 32, 931 (1971)].

[24] A. I. Ansel'm, Vvedenie v teoriyu poluprovodnikov, (Introduction to the Theory of Semiconductors), Fizmatgiz, M., 1962.

Translated by A. Tybulewicz
104